ISSN 0010-9525, Cosmic Research, 2010, Vol. 48, No. 6, pp. 485–500. © Pleiades Publishing, Ltd., 2010.
Original Russian Text © Yu.I. Yermolaev, I.G. Lodkina, N.S. Nikolaeva, M.Yu. Yermolaev, 2010, published in Kosmicheskie Issledovaniya, 2010, Vol. 48, No. 6, pp. 499–515.

Statistical Study of Interplanetary Condition Effect on Geomagnetic Storms

Yu. I. Yermolaev, I. G. Lodkina, N. S. Nikolaeva, and M. Yu. Yermolaev

Space Research Institute, Russian Academy of Sciences, Moscow, Russia

E-mail: yermol@iki.rssi.ru

Received August 27, 2009

Abstract—Based on the archive OMNI data for the period 1976–2000 an analysis has been made of 798 geomagnetic storms with $D_{st} < -50$ nT and their interplanetary sources—large-scale types of the solar wind: CIR (145 magnetic storms), Sheath (96), magnetic clouds MC (62), and Ejecta (161). The remaining 334 magnetic storms have no well-defined sources. For the analysis, we applied the double method of superposed epoch analysis in which the instants of the magnetic storm beginning and minimum of D_{st} index are taken as reference times. The well-known fact that, independent of the interplanetary source type, the magnetic storm begins in 1–2 h after a southward turn of the IMF ($B_z < 0$) and both the end of the main phase of a storm and the beginning of its recovery phase are observed in 1–2 h after disappearance of the southward component of the IMF is confirmed. Also confirmed is the result obtained previously that the most efficient generation of magnetic storms is observed for Sheath before MC. On the average parameters B_z and E_y slightly vary between the beginning and end of the main phase of storms (minimum of D_{st} and D_{st}^* indices), while D_{st} and D_{st}^* indices decrease monotonically proportionally to integral of B_z and E_y over time. Such a behavior of the indices indicates that the used double method of superposed epoch analysis can be successfully applied in order to study dynamics of the parameters on the main phase of magnetic storms having different duration.

DOI: 10.1134/S0010952510060018

INTRODUCTION

Studying the mechanisms of energy transfer from the solar wind into the magnetosphere and of excitation of magnetospheric disturbances is one of key issues of the solar-terrestrial physics. As has been demonstrated by direct space experiments in the beginning of 1970s, the basic parameter leading to disturbances of the magnetosphere is the negative (southward) B_z component of the interplanetary magnetic field (IMF) (or electric field $E_y = V_x B_z$) [1–4], since in its presence the solar wind energy begins entering the magnetosphere, which leads to changes in existing magnetosphere-ionosphere currents and to generation of new currents changing the magnetic field distribution [5].

As has been demonstrated by numerous investigations, the IMF in the undisturbed solar wind lies in the ecliptic plane, i.e., B_z is close to zero. Only in disturbed types of the solar wind streams B_z can have a considerable value. The interplanetary CME (ICME) with a compression region Sheath before them and the compression region between slow and fast solar wind streams (Corotating Interaction Region, CIR) belong to such types of the solar wind. Therefore, these phenomena have been shown in many papers to be large-scale interplanetary sources of magnetospheric disturbances (see, for example, papers [6–19] and references therein).

Ejecta and Magnetic Clouds (MCs) represent subclasses of ICME, the difference between them being in the fact that MCs possess higher and more regular IMF. In addition to CME intensity on the Sun, the found distinctions between MC and Ejecta can be associated with the spacecraft trajectory relative to the ICME axis [21]. Separation of MC and Ejecta also depends on the choice of selection criteria which are conventional enough. In spite of all these ambiguities of definition, differences in the parameters of MC and Ejecta are substantial [22], for example, the magnetic field magnitude in MC is on average twice higher than that in Ejecta (density and dynamic pressure are higher by a factor of 1.5). It is important to note that the situation, when heliospheric conditions as detected on a spacecraft would essentially differ from those acting upon the magnetosphere, is quite improbable since the dimensions of ICME (a few million kilometers [17, 23]) significantly exceed both transverse dimensions of the magnetosphere and spacecraft distances to the Earth's magnetosphere (several tens of thousand kilometers). In the overwhelming majority of papers devoted to generation of magnetic storms under different conditions in the solar wind no separation into MC and Ejecta was

made. We have performed such a distinction (101 MC and 1128 Ejecta were detected in the period 1976–2000 [23]), and in this paper we analyze these phenomena separately.

Though in the literature it was rather frequently pointed out that Sheath could generate magnetic storms (see, for example, review [7] and references therein), rather recently Sheath has become a subject of separate and more profound studies (see [11, 15, 16, 22, 24–28] and references therein). Moreover, in some papers [9, 15, 16, 29] it was found that during Sheath the process of storm generation turned out to be more efficient than during a magnetic cloud. Nevertheless, in many papers (see, for example, [12, 13, 30, 31]) no separation between ICME and Sheath before ICME is made, therefore, their conclusions refer not to ICME, but rather to a mixture ICME+Sheath with an unknown proportion between components. In the present paper we not only study the role of Sheath in generation of magnetic storms, we do this separately for Sheath before MC and before Ejecta.

Experimental results testify the magnetospheric activity to be different for different types of interplanetary streams having served as sources of these disturbances [12–14, 18, 30–33]. This can be associated with a necessity of accounting for the influence of other (in addition to B_z component of the IMF and electric field E_y) parameters of the solar wind, dynamics of parameter variation, and different mechanisms of generating the magnetospheric disturbances at different types of the solar wind.

In many papers attempts were made to compare the extreme values of D_{st} and K_p indices with minimum values of the IMF's B_z component and convective electric field E_y. However, one fails to find any significant distinctions in the above dependences for various types of the solar wind [17]. This peak-to peak approach compares only separate extreme points in the process development, not taking into account the very dynamics of the magnetic storm generation process. Therefore, the approaches using the method of superposed epoch analysis (SEA) turned out to be more fruitful, since this method allows one to study the most typical variations of parameters with time (see Table 1). Frequently, when this method is used, there are the same drawback that were indicated above: (1) no selection in the types of interplanetary sources is made [34–37], (2) no separation in ICME and Sheath is made [12, 13, 30, 31], and (3) ICMEs are not separated into MC and Ejecta [12, 13, 30, 31]. Some papers do not take into account the fact that durations of geoeffective types of the solar wind streams are substantially shorter than the duration of magnetic storms (for example, in recent paper [17] it has been shown that the durations of Sheath, MC, and CIR generating magnetic storms with $D_{st} < -60$ nT in the period 1976–2000 were equal to 9 ± 4 h (for 22 events), 28 ± 12 h (113), and 20 ± 8 h (121), respectively), and parameters of the solar wind for CIR, Sheath, and MC/Ejecta are presented on the intervals 4 to 10 days [19, 31, 33, 38, 39]. In our opinion such approaches are incorrect and lead to incorrect conclusions, since the results obtained refer to a mixture (usually with unknown proportion) of several types of solar wind streams rather than to the indicated type. We tried to take into account all the above-mentioned drawbacks of approaches and methods used previously.

One of key issues of using the SEA is the choice of a reference point (time "0" or the epoch beginning), i.e., of that instant of the process relative to which the time series of several homogeneous phenomena are superposed [11, 17, 37]. This choice has an essential effect on results of investigations, since, strictly speaking, the results of applying SEA are valid only near the epoch beginning because durations of processes can be substantially different even for selected homogeneous phenomena. In most papers that apply SEA for studying magnetic storms (see Table 1) the minimum of D_{st} index (maximum of K_p) was used as zero time [31, 35, 41, 44]. This choice allows one to study the end of the main phase of a storm and the recovery phase beginning. However, using it one cannot investigate interplanetary causes of magnetic storm onset, since the duration between the beginning and end of the storm main phase can change from 2 to 15 h at the average duration of about 7 h [11, 16, 47, 48], and at superposition of the time series according to a minimum of D_{st} index (maximum of K_p) inside the interval of duration of a few hours about −7 h from zero time the parameters belonging to the times before the storm onset and after it are averaged. Nevertheless, such an approach was used in some papers (see Table 1). The choice of the storm onset as a zero time for SEA allows one to investigate the causes of magnetic storms and the initial phase of storm development near the onset. This approach has shown, for example, that storms generated by Sheath have the main phase more steep than the storms generated by other types of the solar wind [16, 18].

The present paper has a definite method-adjustment character, since, in order to investigate the dynamic relation between development of parameters in interplanetary sources and in the magnetospheric indices we apply in this paper the method of double superposed epoch analysis (DSEA). Two reference times are used in this method: we put together the time series according to the storm onset (time "0") and time of D_{st} index minimum (time "6"), the data between them we compress or expand in such a way that durations of the main phases of all magnetic storms would be equal to each other (one can assume

Table 1. The list of papers using the method of superposed epoch analysis with the results obtained in them on interplanetary conditions leading to magnetic storms

N	Number (Years)	Zero time	Selection	SW and IMF	Reference
1	538(1963–1991)	storm onset	no	$B, B_x, B_y, B_z, V, T, n, P_d$	[40]
2	120(1979–1984)	minimum of D_{st}	no	B_z, n, V	[41]
3	150(1963–1987)	return B_z	no	B_z, P_d	[42]
4	305(1983–1991)	storm onset	no	B_z, P_d	[43]
5	1085(1957–1993)	minimum of D_{st}	D_{st}	B_z, P_d	[44]
6	130(1966–2000)	storm onset	no	$B, B_x, B_y, B_z, \|B_x\|, \|B_y\|, \|B_z\|, V, n, P_d$	[45]
7	623(1976–2000)	storm onset and minimum of D_{st}	types[a] of SW	$B, B_x, B_y, B_z, V, T, n, P_d, nkT, \beta, T/T_{ex}$	[11, 15, 16, 46]
8	78(1996–2004)	minimum of D_{st}	types[b] of SW	$B, B_z, dB/B, V, T, n$	[38]
9	549(1974–2002)	minimum of D_{st}	yes[c]	$B, B_x, B_y, B_z, \|B_x\|, \|B_y\|, \|B_z\|, B_s, VB_s, V, T, n, P_d$	[35]
10	623(1976–2000)	storm onset	types[a] of SW	$\sigma B, \sigma V, \sigma T, \sigma n$	[17]
11	28(1997–2002)	storm onset and minimum of D_{st}	types[d] of SW	B_z, P_d, V, E_y	[18]
12	10(2004)	storm onset	no	$B_x, B_y, B_z, B, \varepsilon, V, n, P_d, M_a, E_y$	[19]
13	71(2000–2006)	minimum of D_{st}	types[b] of SW	B_z, V_x, V_y, P_d	[31]
14	29(1999–2002)	storm onset main phase, minimum of D_{st}	no	B_z, P_d	[37]

[a] – (1) CIR, (2) Sheath и (3) MC; [b] – (1) CIR и (2) MC (Sheath + MC);
[c] – (1) moderate storm at solar minimum, (2) moderate storm at solar maximum, (3) strong storm at solar minimum and (4) strong storm at solar maximum.
[d] – (1) MC и (2) Sheath.

that in [43] a similar approach is used, however incomplete is its description). As a storm onset we take the first one-hour point in which a sharp drop of the D_{st} index is observed, and for the analysis we take all storms with $D_{st} \le -50$ nT (while only storms with $D_{st} \le -60$ nT were analyzed in our previous similar works [11, 15–17]). Such an approach allows us to investigate simultaneously the interplanetary conditions leading to the beginning and end of the storm main phase, as well as their dynamics throughout the entire main phase of the storm.

Thus, unlike the previous works, the present paper includes the following new elements of the method:

1) A larger number of the types of interplanetary sources of magnetic storms is used, including separate analysis of Sheath and ICME, separation of ICME into Ejects and magnetic clouds (MC), and two types of Sheath between them.

2) The doubled method of superposed epoch analysis is used, the instants of magnetic storm onset and D_{st} index minimum being taken as reference times.

METHOD

In total, 798 moderate and strong magnetic storms with intensity $D_{st} \le -50$ nT were detected for the entire period 1976–2000. But only for 464 magnetic storms (i.e., for 58% of all magnetic storms) corresponding events in the solar wind were identified. The sources of remaining 334 magnetic storms (i.e., 42% of 798 storms) turn out to be undetermined. Basically, this is due to the absence of data on plasma and IMF, which makes it impossible to identify the solar wind type for a given period. The method of identifying the large-scale types of the solar wind is described in detail in our paper [22]. It consists in comparison of every point of

the OMNI database with a set of threshold criteria for key parameters of the solar wind and IMF. It is assumed that an event in the solar wind results in a magnetic storm if the D_{st} minimum falls inside the event interval or follows after it during no more than 2 hours. Our analysis has shown that 145 magnetic storms were caused by CIR events; 96 magnetic storms were produced by Sheath (12 magnetic storms were generated by Sheath before MC, Sh_{MC}, and 84 magnetic storms—by Sheath before Ejecta, Sh_E); 62 magnetic storms are associated with magnetic clouds MC (50 storms being caused by MC with Sheath and 12 by MC without Sheath); and 161 magnetic storms were associated with Ejecta events (115 Ejecta with Sheath and 46 Ejecta without Sheath).

The data for the intervals selected according to the solar wind types were processed using the method of superposed epoch analysis with two check-point times: the time of magnetic storm onset (time "0") and the time of D_{st} index minimum (time "6"). The interval from time "0" to time "6" contains artificially changed durations of events; therefore, these times are taken in quotation marks to distinguish them from really measured time. The first 1-hour point of a sharp decrease of the D_{st} index was taken as the magnetic storm "onset" [15–17]. For all events (intervals) the time scale between these times was divided in 5 subintervals with equal relative durations, and the data in one subinterval were averaged in accordance with the number of points fell in this subinterval (their number can be different in different subintervals). This procedure means that the time scale for real data in the range between points "0" and "6" was varied in a linear way, though this variation was small (for 2/3 of events the duration has changed by no more than 1/3), since the duration of the storm main phase is equal, on average, to 7 ± 4 h [15–17]. The time scale before time "0" and after time "6" has remained unchanged. The advantage of this method is a possibility to compare dynamics of interplanetary and magnetospheric parameters during the main phases of magnetic storms having different durations.

In accordance with SEA, the data were averaged over intervals from −12 to +24 h, the duration of each interval of a given type of the solar wind being taken into account. According to our results, durations of different types of the solar wind for the period 1976–2000 were equal to: 20.6 ± 12.2 h for CIR, 29.8 ± 20.5 h for Ejecta, 28.2 ± 13.4 h for MC, and 15.7 ± 10.1 h for Sheath [22]. These values are close to average durations of these types of the solar wind having resulted in magnetic storms [15–17]. Therefore, the number of points in averaging intervals drops down substantially (the error increases accordingly) to the edges of chosen intervals from −12 to +24 h, especially for Sheath. Low statistics for some parts of the curves presented in the figures reveals itself in their noticeable indentation. The errors (standard deviations) in the interval from −12 to +12 h are close to those presented in our paper [17]. Therefore, we have checked statistical significance for the statements formulated below, and in some cases, when discussing results for which a hypothesis has no desired statistical significance, we say only about possible tendencies that require further investigations.

RESULTS

The results of our analysis are presented as 16 figures (each for one of 16 different parameters of the solar wind and magnetospheric indices) and Tables 2–4 that show for every type of the solar wind the mean values with variances for 16 parameters at time instants "0" and "6" and allow one to estimate their gradients in this time interval. Distinctions between Tables 2–4 consist in the fact that in Table 2 the data are presented for the total range of the D_{st} index less than −50 nT, while in Tables 3 and 4 the data are divided into moderate storms with $-100 < D_{st} \le -50$ nT and strong storms with $D_{st} \le -100$ nT. Due to a lack of space we do not present figures with selection of data according to the D_{st} index value. All Figs. 1–16 have the identical structure and show dynamics of 16 parameters on 8 panels for 8 different types of the solar wind: magnetic clouds MC, Ejecta, the sum of two types MC + Ejecta, CIR, Sheath before MC, Sheath before Ejecta, and the sum of both types of Sheath and the indeterminate type. The number of events included into processing for every type of the solar wind is shown in the figure. The solid black central line shows the behavior of the mean value, while the upper and lower lines (for some parameters these lines presented in logarithmic scale can be interrupted or absent altogether) represents the mean value with added or subtracted variance. Dashed gray line shows the behavior of a parameter for all types of the solar wind (i.e., without selection according to solar wind types), and this line allows one to compare the behavior of a given type of the solar wind with a certain "mean" behavior.

Figures 1 and 2 present the dynamics of standard D_{st} and corrected D_{st}^* indices, respectively. Since it is just according to D_{st} index that we selected events, for all types of the solar wind in the range of time "0–6" a monotonic decrease of both the indices is observed. The steepest change of the indices is observed for Sheath before MC. For MC and Sheath before MC the D_{st} index goes lower than the curve for "all", while for CIR is higher, i.e., magnetic storms generated by MC and Sheath before MC are stronger, on the average, while CIR-generated storms are weaker than the average. The behavior of D_{st}^* is the same as for D_{st}, but, generally, distinctions from "all" have become smaller.

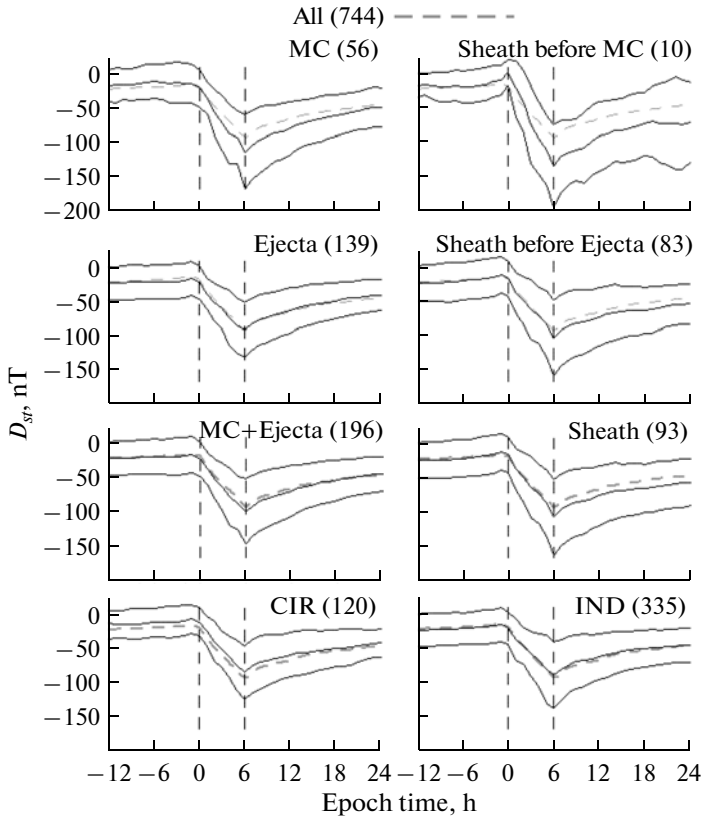

Fig. 1. Dynamics of the D_{st} index behavior for different types of the solar wind (see text).

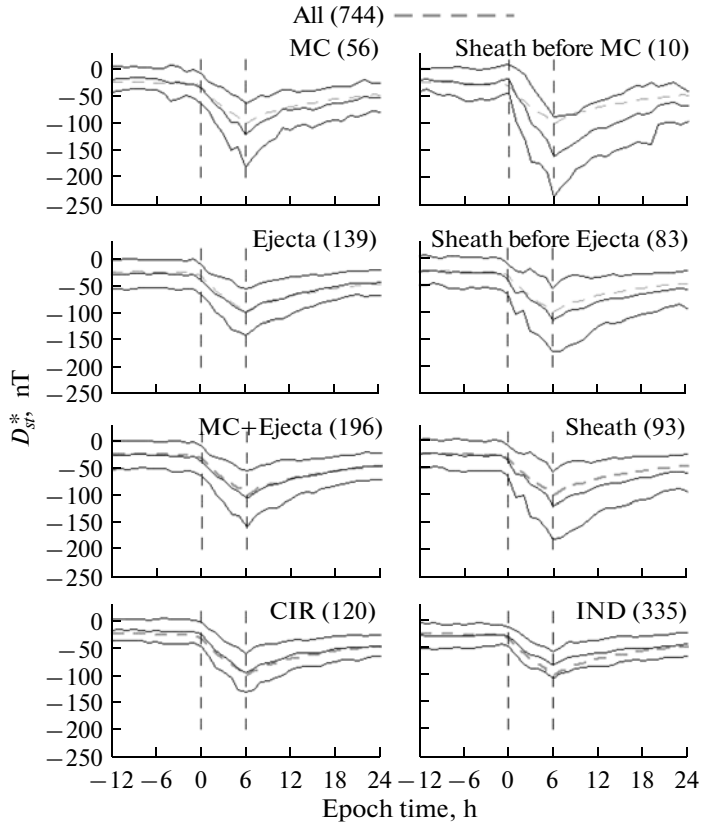

Fig. 2. The same as in Fig. 1, but for corrected index D^*_{st}.

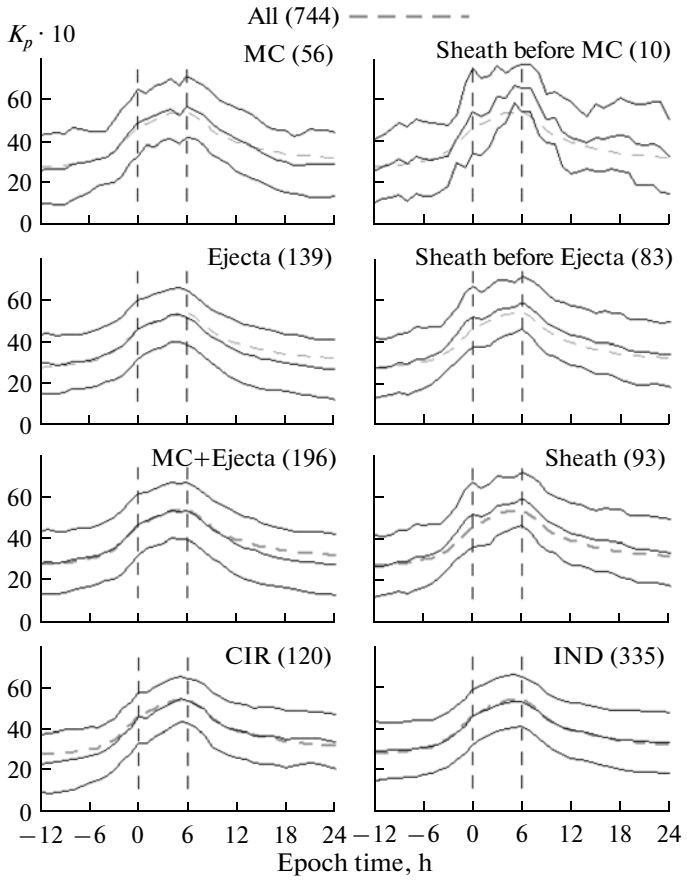

Fig. 3. The same as in Fig. 1 for the K_p index.

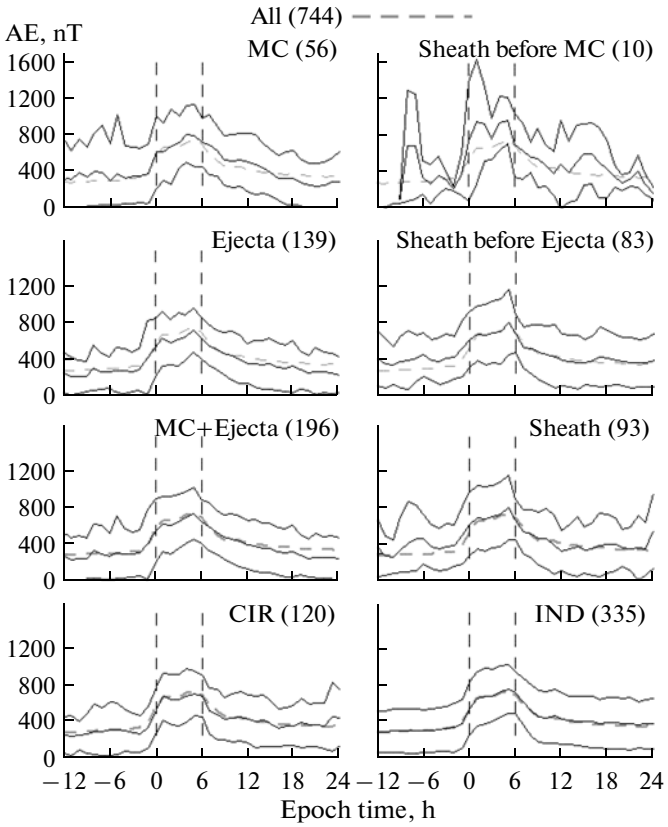

Fig. 4. The same as in Fig. 1 for the *AE* index.

Figures 3 and 4 demonstrate the time behavior of K_p and *AE* indices. Unlike D_{st} and D_{st}^* indices, the K_p and *AE* indices for all types of the solar wind begin growing 3–5 h prior to time "0" and decrease slowly after time "6". Activity in both these indices for all types of the solar wind weakly increase within the interval "0–6", and reaches its maximum near time "6". In K_p index, the activity for MC and Sheath is higher than for "all" types, while in *AE* index the activity is higher only for Sheath before MC.

The behavior of bulk velocity *V* of the solar wind is shown in Fig. 5. The velocity increases near time "0" for all types of the solar wind. For MC, Ejecta, and "indeterminate" types *V* is invariable in the range "0–6", while for CIR and Sheath it increases. For MC, Ejecta, and Sheath the velocity drops down after time "6", for "indeterminate" type it is invariable and for CIR increases. In the range "0–6" for MC, Ejecta, and "indeterminate" types the value of *V* is close to the curve for "all", for CIR and Sheath it is lower and higher, respectively.

The behavior of proton temperature *T* and relative temperature T/T_{ex} (T_{ex} is temperature estimated through velocity based on the mean dependence of temperature and the solar wind velocity [22]) is shown in Figs. 6 and 7. The absolute and relative temperatures for CIR and all types of Sheath increase for 3–5 h before time "0" and are invariable for all other types of the solar wind. In the range "0–6" *T* drops for MC and Ejecta, increasing for all other types. T/T_{ex} also drops for MC and Ejecta, it increases for CIR and slightly changes for the remaining types. For time exceeding "6" both temperatures drop for CIR and all types of Sheath, and there are but small changes for other of solar wind types. Both the temperatures are lower than the mean curve for MC and Ejecta, higher for CIR, and have small distinctions for "indeterminate" type.

Figure 8 presents the time behavior of ion density *n* in the solar wind. For all types of the solar wind *n* begins to increase several hours prior to time "0". After time "6" *n* remains invariable for MC, Ejecta, and "indeterminate" types, while it continues to decrease for CIR and Sheath. Density *n* reaches its maximum about time "0" and drops to time "6" for all types of the solar wind. For MC, Ejecta, and "indeterminate" type *n* is lower than the curve for "all", while in case of CIR and Sheath it is higher.

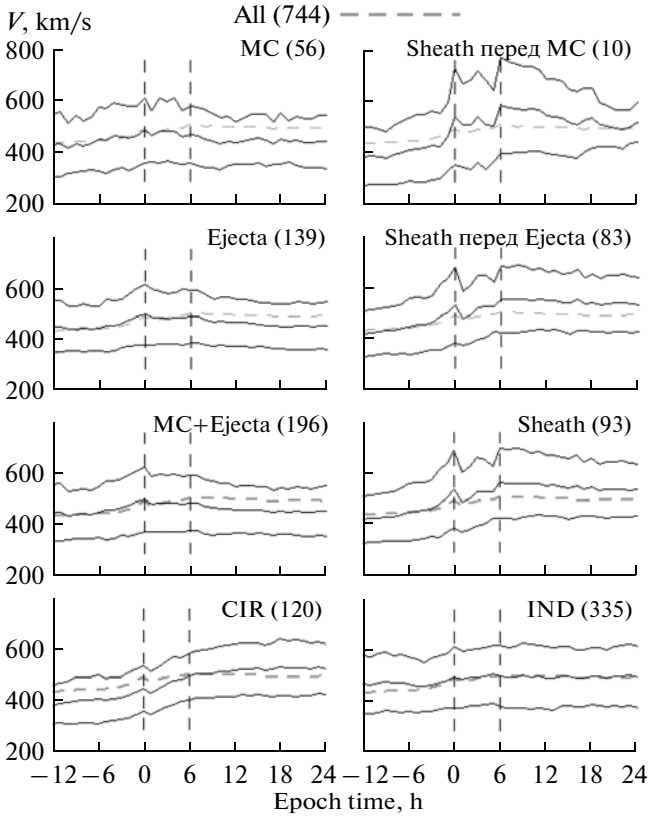

Fig. 5. The same as in Fig. 1 for the bulk velocity V of the solar wind.

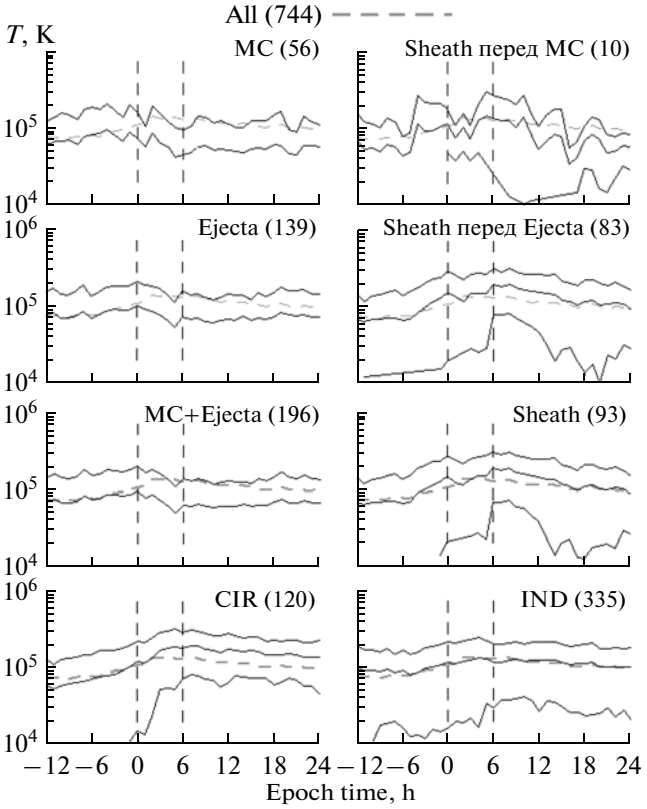

Fig. 6. The same as in Fig. 1 for the proton temperature T of the solar wind.

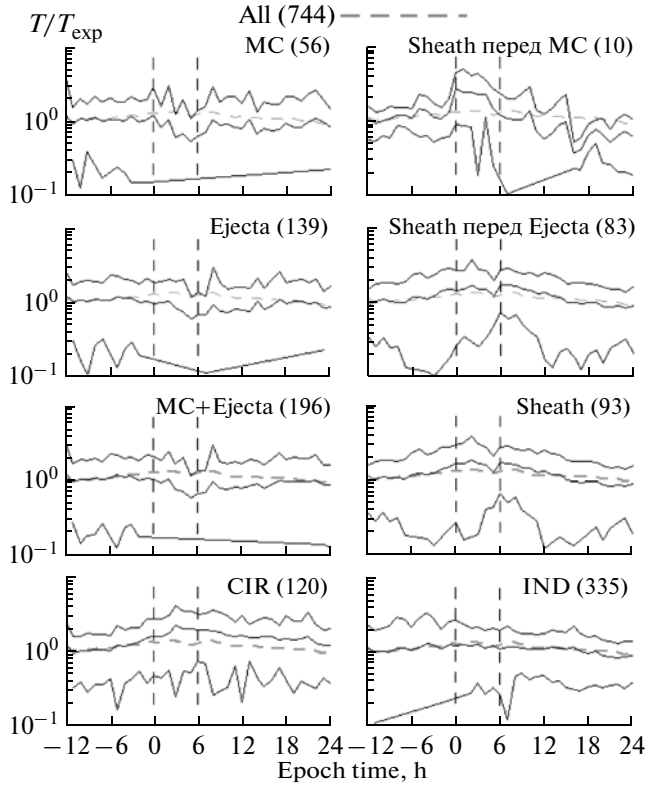

Fig. 7. The same as in Fig. 1 for the relative temperature T/T_{ex} of the solar wind.

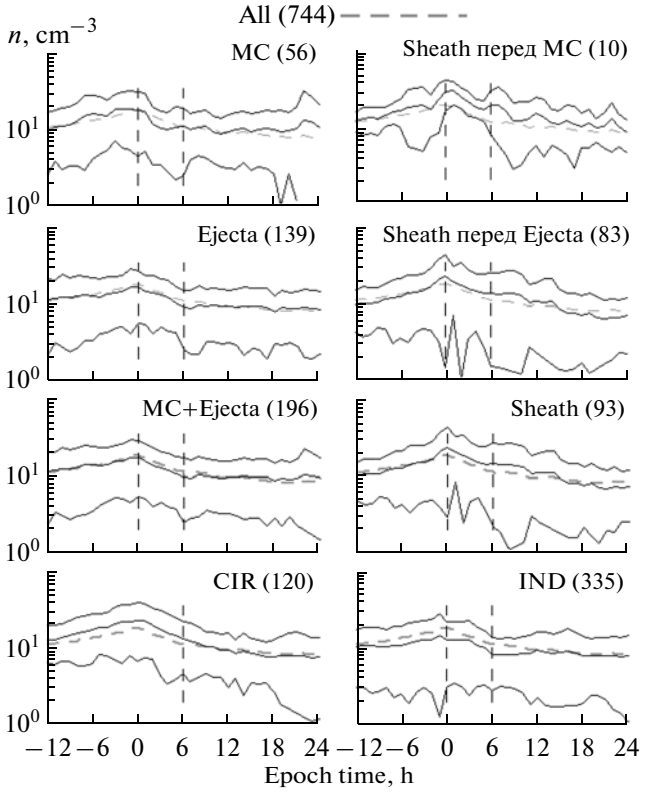

Fig. 8. The same as in Fig. 1 for the ion density n of the solar wind.

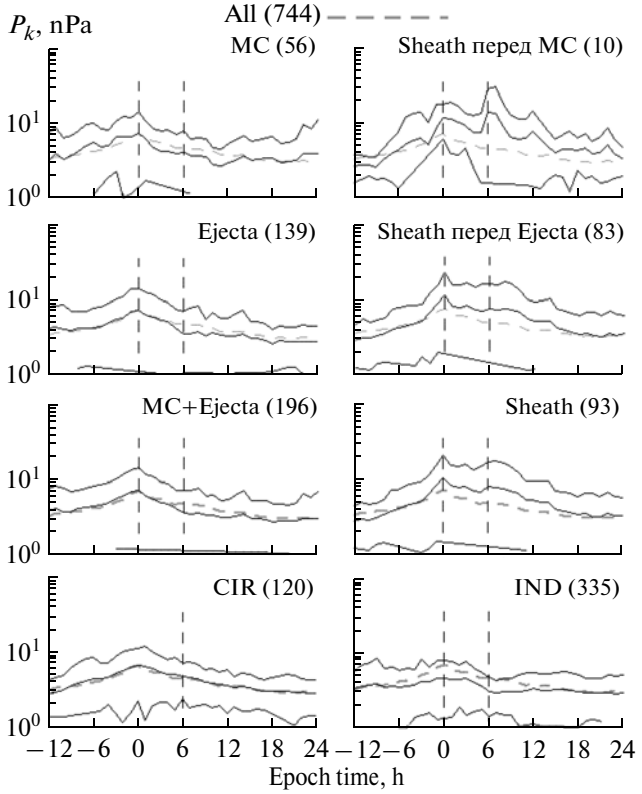

Fig. 9. The same as in Fig. 1 for the dynamic pressure P_k of the solar wind.

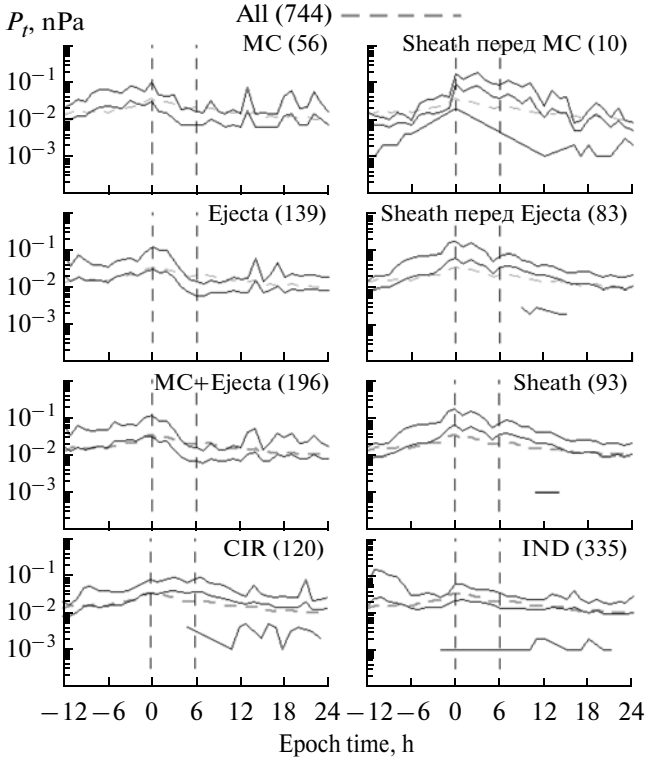

Fig. 10. The same as in Fig. 1 for the thermal pressure P_t of the solar wind.

The time behavior of dynamic (P_k) and thermal (P_t) pressures of the solar wind is presented in Figs. 9 and 10. The dynamic pressure behavior completely repeats that of density n in Fig. 8. The thermal pressure also behaves itself similar to density dynamics with one exception: for CIR thermal pressure does not change in the time interval "0–6".

Figure 11 shows the dynamics of magnitude B of the interplanetary magnetic field. For all types of the solar wind B begins increasing several hours prior to time "0" (for Sheath before MC a strong enhancement by 10 nT is observed 1 h before time "0"), reaches a maximum in the range "0–6" and then slowly decreases with time.

For types CIR, all Sheath, "indeterminate", and "all" there is a tendency in the range "0–6" to a decrease of B with the course of time. The curves of B for MC, CIR, and all Sheath are higher than for "all" type, while those for "indeterminate" type are lower.

Figures 12 and 13 show the B_x and B_y components of the IMF. With an exception of Sheath before MC in all types of the solar wind B_x and B_y change slightly near zero values over the entire interval from −12 to 24 h. For Sheath before MC B_x drops strongly 1 h before time "0" and then increases near time "6" up to a value of the "all" type. After that time it oscillates with a large amplitude in the region of negative values. The B_y component of this type of the wind has positive values at −6 h and negative values at −2 h. About time "0" it assumes zero values, and further increases up to a value of about 10 nT near time "6". Next, during 12 h it slowly drops down to zero values.

As is well known, for exciting magnetic storms the most critical are the B_z component of the IMF and E_y component of the electric field, both of them are shown in Figs. 14 and 15. For all types of the solar wind these parameters have zero values long before time "0", 1–3 h before it they take on negative values, slightly change in the interval "1–5", begin increasing in the interval "5–6" and reach zero values, further being kept constant (only for Sheath before MC they have positive values for time exceeding "6"). For MC and Sheath before MC the values of B_z and E_y are lower than for "all" type, for all other types their values are the same as for the "all" type.

Figure 16 shows the behavior of β-parameter (ratio of thermal and magnetic pressures). 1–2 h prior to time "0" β drops down for MC and Ejecta and increases for CIR and Sheath. In the time interval "0–6" for MC and Ejecta β decreases with time, while for CIR and Sheath before MC it increases, and for other types remains invariable. For MC and Ejecta β is lower

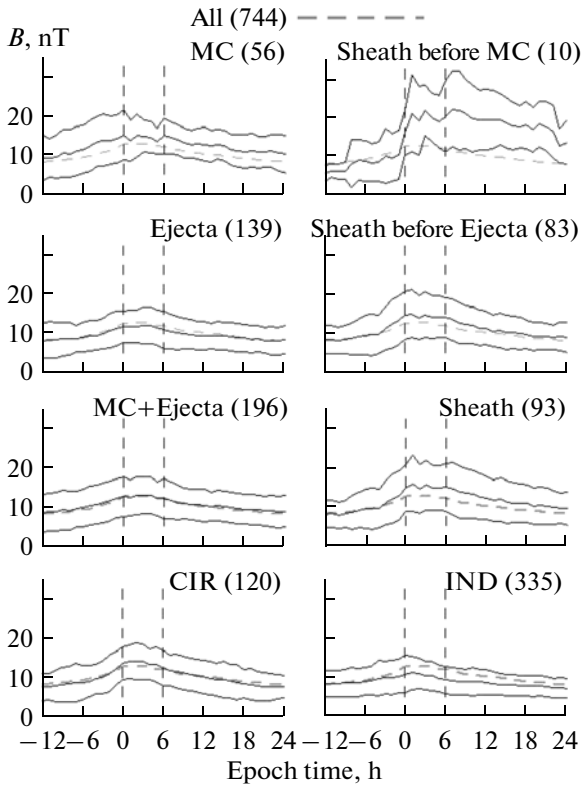

Fig. 11. The same as in Fig. 1 for the interplanetary magnetic field magnitude, B.

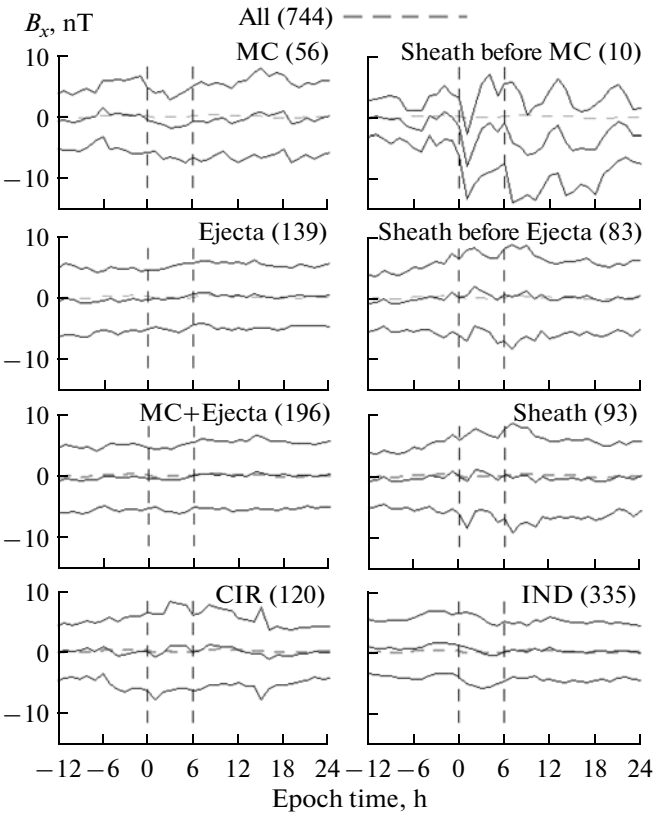

Fig. 12. The same as in Fig. 1 for the B_x component of the interplanetary magnetic field.

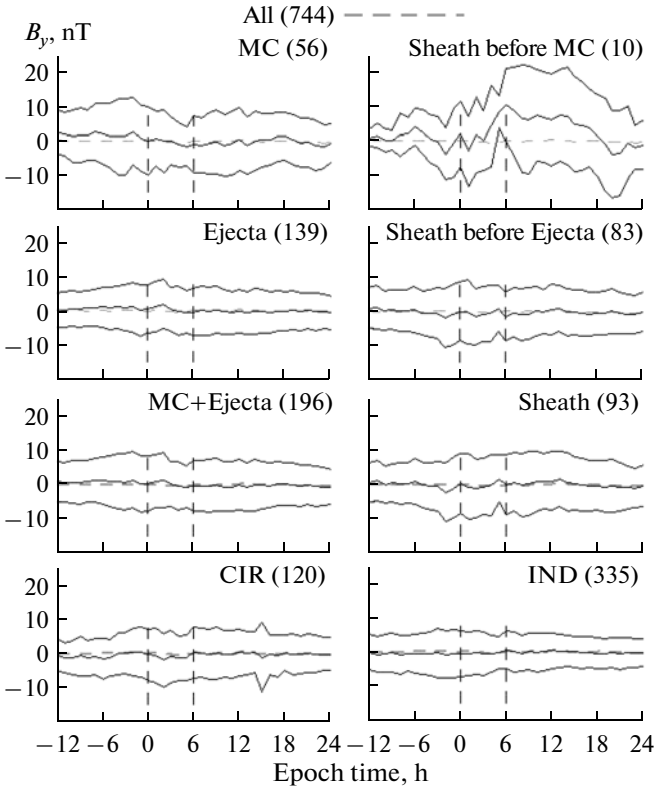

Fig. 13. The same as in Fig. 1 for the B_y component of the interplanetary magnetic field.

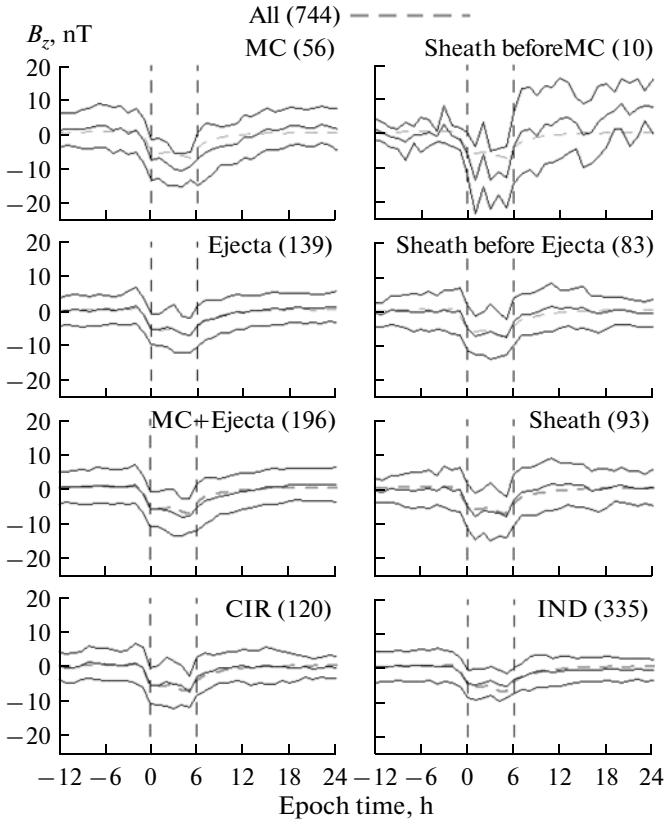

Fig. 14. The same as in Fig. 1 for the B_z component of the interplanetary magnetic field.

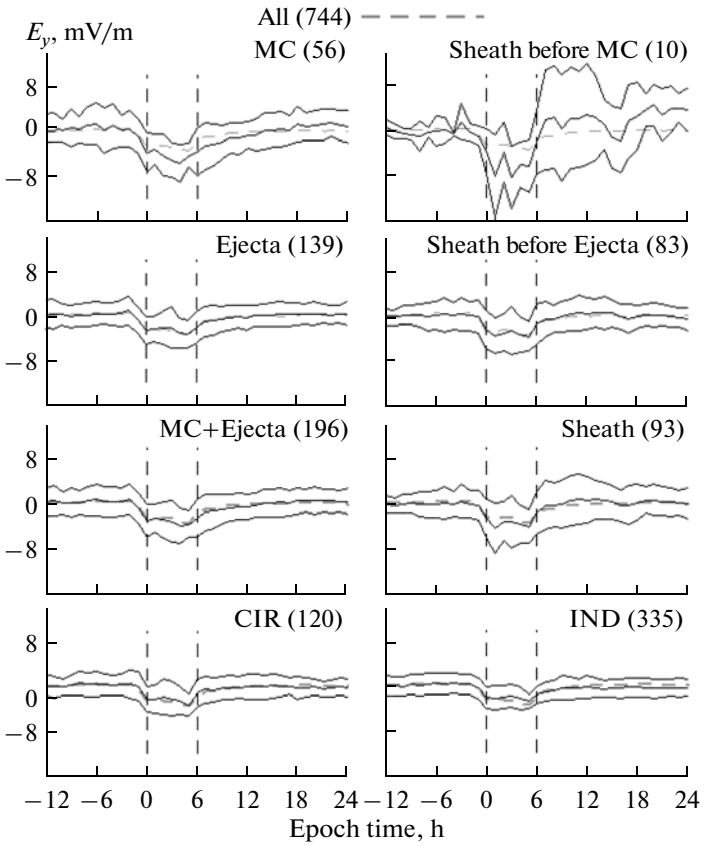

Fig. 15. The same as in Fig. 1 for the electric field E_y.

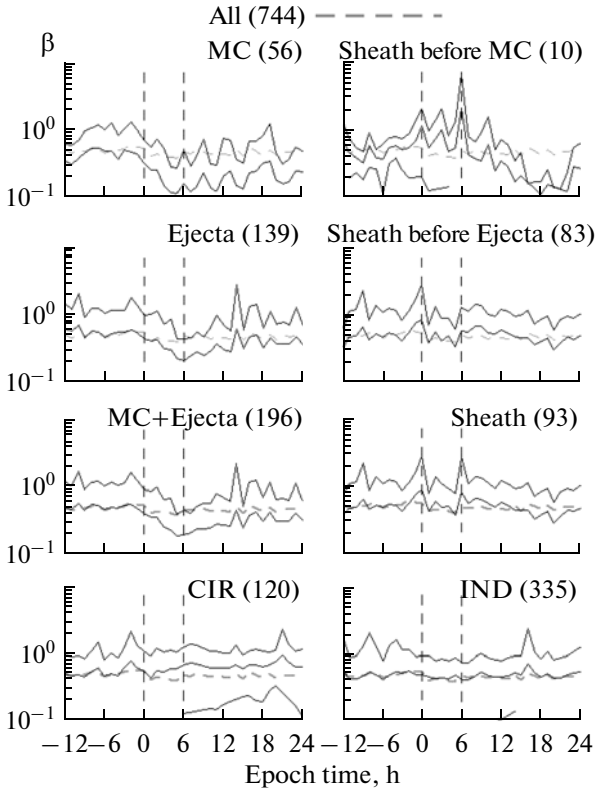

Fig. 16. The same as in Fig. 1 for parameter β (the ratio of thermal and magnetic pressures).

than the curve for "all", while for CIR and Sheath before MC it is higher.

The data presented in Figs. 1–16 are summarized in Table 2. For different interplanetary sources of magnetic storms with $D_{st} \le -50$ nT this table presents mean values and variances for a number of parameters of the solar wind, IMF, and magnetospheric indices at instants "0" and "6" (see columns designated as "0" and "6"). The values presented in Table 2 give quantitative estimates of those specific features that were qualitatively discussed above when the figures were analyzed.

We have made a similar analysis separately for moderate ($-100 < D_{st} \le -50$ nT) and strong ($D_{st} \le -100$ nT) storms. Because of the lack of space we do not present all figures, however, the data obtained are presented in Tables 3 and 4. The structure of Tables 3 and 4 is similar to the structure of Table 2. Qualitatively, Tables 3 and 4 repeat the results of Table 2 and Figs. 1–16. However, it should be noted that capability of more efficient generation of magnetic storms by the Sheath region (in comparison with other interplanetary sources) reveals itself more strongly for strong magnetic storms with $D_{st} \le -100$ nT (higher gradient for Sheath). The fact also engage our attention that at generation of stronger storms most parameters stronger deviate from mean parameters than for weak and moderate storms, independent of the type of interplanetary source. This conclusion sounds trivially in its general form, but the question of particular parameters influencing this fact remains open. This tendency will be described in more detail in our subsequent publications.

DISCUSSION

Since this paper deals mainly with the issues of method, it is necessary to note that the method of double SEA, apparently, used for the first time for this type of analysis allows one to reproduce earlier obtained results. First of all this is the fact that, independent of the type of interplanetary source the magnetic storm begins in 1–2 h after the IMF turn to the south ($B_z < 0$), while both the end of the storm main phase and beginning of the recovery phase are observed in 1–2 h after drop of the IMF southward component. Since the method used does not changes the time scale of data prior to the magnetic storm onset for SEA with epoch time equal to the storm onset, then the data obtained in this time interval well agree both with previous results obtained by other authors under appropriate data selection according to types of interplanetary sources or without such a selection (see corresponding references in Table 1) and with our previous results [15–17]. Due to analogous reasons, the results obtained agree with corresponding previous results in

Table 2. Mean values and deviations for all events with $D_{st} \le -50$ nT

Parameter	IND		CIR		Ejecta		MC		Sheath		MC+Ejecta	
	$t=0$	$t=6$	$t=0$	$t=6$	$t=0$	$t=6$	$t=0$	$t=6$	$t=0$	$t=6$	$t=0$	$t=6$
D_{st}, nT	−20.4 ± ± 23.4	−89.2 ± ± 48.5	−9.2 ± ± 20.2	−85.5 ± ± 39.8	−27.9 ± ± 22.4	−92.2 ± ± 39.4	−23.5 ± ± 34.2	−116.3 ± ± 54.8	−14.3 ± ± 26.2	−104.9 ± ± 55.2	−26.4 ± ± 26.5	−100.0 ± ± 47.8
D^*_{st}, nT	−29.7 ± ± 17.2	−81.8 ± ± 24.9	−25.7 ± ± 20.5	−95.8 ± ± 34.9	−39.7 ± ± 26.6	−99.3 ± ± 41.8	−35.7 ± ± 29.2	−124.2 ± ± 59.4	−39.0 ± ± 28.2	−118.1 ± ± 60.0	−38.5 ± ± 27.2	−107.7 ± ± 52.0
$K_p \cdot 10$	46 ± ± 14	53 ± ± 12	47 ± ± 12	54 ± ± 11	42 ± ± 13	52 ± ± 12	50 ± ± 18	57 ± ± 15	54 ± ± 15	59 ± ± 13	44 ± ± 15	54 ± ± 14
B_x, nT	1.2 ± ± 5.2	0.1 ± ± 5.0	0.5 ± ± 6.3	−0.2 ± ± 6.1	0.02 ± ± 4.9	0.7 ± ± 5.1	−1.3 ± ± 5.5	−0.9 ± ± 5.8	0.1 ± ± 6.3	0.7 ± ± 7.2	−0.4 ± ± 5.1	0.2 ± ± 5.4
B_y, nT	−0.5 ± ± 6.7	0.5 ± ± 5.5	−0.1 ± ± 7.5	0.4 ± ± 7.5	−0.5 ± ± 6.0	−0.3 ± ± 6.9	0.6 ± ± 10.6	−0.6 ± ± 8.3	−0.2 ± ± 8.7	−0.4 ± ± 8.4	−0.3 ± ± 7.8	−0.4 ± ± 7.3
B, nT	10.7 ± ± 4.8	9.3 ± ± 3.5	13.7 ± ± 4.3	12.5 ± ± 4.5	10.5 ± ± 2.8	10.9 ± ± 4.9	16.2 ± ± 5.9	14.9 ± ± 4.6	15.0 ± ± 6.3	14.4 ± ± 5.6	12.3 ± ± 4.8	12.1 ± ± 5.1
B_z, nT	−4.6 ± ± 4.0	−3.4 ± ± 3.7	−5.5 ± ± 5.346	−2.8 ± ± 5.7	−5.1 ± ± 3.9	−4.4 ± ± 5.9	−9.1 ± ± 5.8	−7.4 ±7.9	−4.5 ± ± 6.7	−2.8 ± ± 7.1	−6.4 ± ± 5.0	−5.3 ± ± 6.7
n, cm^{-3}	12.5 ± ± 9.6	8.2 ± ± 5.4	23.5 ± ± 16.4	13.3 ± ± 8.7	13.4 ± ± 7.5	9.0 ± ± 6.4	14.6 ± ± 10.6	11.5 ± ± 8.8	24.3 ± ± 21.3	14.3 ± ± 12.1	13.6 ± ± 8.4	9.7 ± ± 7.2
V, km/s	496 ± ± 120	499 ± ± 121	448 ± ± 93	494 ± ± 91	470 ± ± 100	494 ± ± 103	498 ± ± 153	469 ± ± 115	541 ± ± 148	558 ± ± 138	476 ± ± 117	487 ± ± 107
P_k, nPa	4.7 ± ± 3.3	3.1 ± ± 1.6	7.2 ± ± 4.7	5.0 ± ± 2.5	5.0 ± ± 4.1	3.5 ± ± 3.3	7.0 ± ± 6.9	4.2 ± ± 3.7	11.6 ± ± 10.7	7.9 ± ± 9.3	5.5 ± ± 5.0	3.7 ± ± 3.4
T, K 10^5	1.2 ± ± 1.0	1.1 ± ± 0.8	1.3 ± ± 1.1	1.8 ± ± 1.1	0.5 ± ± 0.6	0.7 ± ± 0.8	0.8 ± ± 1.1	0.4 ± ± 0.5	1.7 ± ± 1.3	1.9 ± ± 1.2	0.6 ± ± 0.8	0.6 ± ± 0.8
P_t, 10^{-2} nPa	2.1 ± ± 3.6	1.3 ± ± 2.0	3.8 ± ± 0.041	3.7 ± ± 4.8	0.9 ± ± 0.010	0.6 ± ± 0.7	1.2 ± ± 1.3	0.7 ± ± 1.0	7.0 ± ± 11.0	3.6 ± ± 3.6	1.0 ± ± 1.1	0.7 ± ± 0.8
β	0.48 ± ± 0.44	0.40 ± ± 0.33	0.58 ± ± 0.566	0.68 ± ± 0.5	0.21 ± ± 0.18	0.20 ± ± 0.22	0.14 ± ± 0.13	0.16 ± ± 0.34	0.96 ± ± 2.09	0.78 ± ± 1.89	0.19 ± ± 0.17	0.19 ± ± 0.27
T/T_{ex}	1.20 ± ± 1.44	1.11 ± ± 0.84	1.67 ± ± 1.11	1.96 ± ± 1.20	0.65 ± ± 0.63	0.68 ± ± 0.69	0.94 ± ± 1.25	0.57 ± ± 0.73	1.67 ± ± 1.22	1.70 ± ± 1.05	0.74 ± ± 0.85	0.65 ± ± 0.70
E_y, mV/m	−1.99 ± ± 1.88	−1.57 ± ± 1.49	−2.28 ± ± 2.40	−1.05 ± ± 2.47	−2.43 ± ± 2.0	−2.02 ± ± 2.87	−4.63 ± ± 3.69	−3.58 ± ± 4.39	−2.51 ± ± 3.67	−1.40 ± ± 3.72	−3.06 ± ± 2.78	−2.48 ± ± 3.46
AE, nT	529.2 ± ± 291.5	707.9 ± ± 230.4	516.1 ± ± 253.2	674.1 ± ± 227.4	518.2 ± ± 316.3	622.1 ± ± 225.6	598.5 ± ± 398.0	705.8 ± ± 264.3	619.8 ± ± 345.8	671.2 ± ± 224.9	543.2 ± ± 345.8	646.2 ± ± 240.4

Table 3. Mean values and deviations for $-100 < D_{st} \le -50$ nT

Parameter	IND		CIR		Ejecta		MC		Sheath		MC + Ejecta	
	$t=0$	$t=6$	$t=0$	$t=6$	$t=0$	$t=6$	$t=0$	$t=6$	$t=0$	$t=6$	$t=0$	$t=6$
D_{st}, nT	−18.1 ± ± 19.6	−71.1 ± ± 13.5	−6.3 ± ± 17.6	−70.2 ± ± 12.6	−24.8 ± ± 16.7	−71.2 ± ± 13.4	−9.1 ± ± 21.8	−72.8 ± ± 12.9	−11.0 ± ± 22.2	−73.7 ± ± 13.6	−21.0 ± ± 19.1	−71.5 ± ± 13.2
D^*_{st}, nT	−30.1 ± ± 16.6	−76.0 ± ± 17.5	−22.8 ± ± 15.3	−82.9 ± ± 15.0	−33.2 ± ± 18.2	−76.6 ± ± 19.3	−24.0 ± ± 17.3	−77.6 ± ± 16.7	−31.7 ± ± 21.9	−89.2 ± ± 18.7	−31.1 ± ± 18.4	−76.8 ± ± 18.7
$K_p \cdot 10$	43 ± ± 12	49 ± ± 10	45 ± ± 11	51 ± ± 9	39 ± ± 10	47 ± ± 10	38 ± ± 12	46.3 ± ± 10.2	49 ± ± 13	54 ± ± 11	39 ± ± 11	47 ± ± 10
B_x, nT	1.1 ± ± 4.8	0.1 ± ± 4.5	0.4 ± ± 5.8	−0.4 ± ± 6.2	0.3 ± ± 5.0	0.5 ± ± 5.3	−1.9 ± ± 3.8	−1.0 ± ± 5.7	0.3 ± ± 5.9	2.1 ± ± 6.7	−0.2 ± ± 4.8	0.1 ± ± 5.4
B_y, nT	−0.7 ± ± 6.0	0.007 ± ± 4.6	0.3 ± ± 7.2	0.5 ± ± 6.6	−1.4 ± ± 5.2	−0.6 ± ± 5.7	3.4 ± ± 6.5	−1.1 ± ± 6.5	−0.4 ± ± 7.0	−2.3 ± ± 6.7	−0.4 ± ± 6.0	−0.8 ± ± 5.9
B, nT	9.8 ± ± 3.6	8.5 ± ± 2.2	13.1 ± ± 4.0	11.8 ± ± 3.8	9.7 ± ± 2.2	9.8 ± ± 4.3	12.1 ± ± 2.6	12.1 ± ± 2.2	13.0 ± ± 5.0	12.9 ± ± 4.5	10.4 ± ± 2.5	10.4 ± ± 4.0
B_z, nT	−4.1 ± ± 3.3	−3.2 ± ± 3.6	−5.0 ± ± 5.3	−2.4 ± ± 5.2	−5.3 ± ± 3.0	−3.5 ± ± 5.6	−5.4 ± ± 3.9	−5.8 ± ± 5.2	−5.0 ± ± 6.3	−1.6 ± ± 5.4	−5.3 ± ± 3.3	−4.1 ± ± 5.6
n, cm^{-3}	10.8 ± ± 7.4	7.7 ± ± 5.2	23.5 ± ± 17.1	12.7 ± ± 9.0	11.7 ± ± 6.9	7.6 ± ± 4.7	9.7 ± ± 3.6	8.7 ± ± 4.1	21.9 ± ± 20.2	11.5 ± ± 7.4	11.2 ± ± 6.3	7.9 ± ± 4.6
V, km/s	496 ± ± 119	500 ± ± 122	444 ± ± 88	488 ± ± 90	448 ± ± 81	476 ± ± 89	411 ± ± 75	432 ± ± 77	502 ± ± 114	521 ± ± 99	437 ± ± 82	466 ± ± 88
P_k, nPa	4.0 ± ± 2.2	2.9 ± ± 1.5	6.9 ± ± 3.6	4.6 ± ± 2.3	3.8 ± ± 2.4	2.6 ± ± 1.4	2.8 ± ± 1.8	2.7 ± ± 1.3	8.7 ± ± 7.8	5.0 ± ± 2.8	3.6 ± ± 2.4	2.6 ± ± 1.4
T, K, 10^5	1.0 ± ± 0.85	1.2 ± ± 0.88	1.4 ± ± 1.12	1.8 ± ± 1.0	0.5 ± ± 0.51	0.8 ± ± 0.95	0.6 ± ± 0.60	0.5 ± ± 0.58	1.7 ± ± 1.38	2.0 ± ± 1.25	0.5 ± ± 0.53	0.7 ± ± 0.89
P_t, 10^{-2} nPa	1.4 ± ± 1.3	1.0 ± ± 1.0	3.9 ± ± 4.2	3.7 ± ± 5.2	0.7 ± ± 0.7	0.6 ± ± 0.7	0.7 ± ± 0.7	0.7 ± ± 1.0	4.5 ± ± 5.1	2.9 ± ± 2.4	0.7 ± ± 0.7	0.6 ± ± 0.7
β	0.47 ± ± 0.43	0.37 ± ± 0.26	0.63 ± ± 0.59	0.65 ± ± 0.55	0.20 ± ± 0.17	0.22 ± ± 0.25	0.14 ± ± 0.11	0.15 ± ± 0.20	0.65 ± ± 0.83	0.61 ± ± 0.77	0.18 ± ± 0.16	0.20 ± ± 0.24
T/T_{ex}	0.96 ± ± 0.65	0.97 ± ± 0.55	1.79 ± ± 1.17	1.98 ± ± 1.23	0.61 ± ± 0.47	0.73 ± ± 0.67	1.19 ± ± 1.51	0.79 ± ± 0.94	1.50 ± ± 0.81	1.69 ± ± 0.95	0.77 ± ± 0.88	0.74 ± ± 0.74
E_y, mV/m	−1.78 ± ± 1.63	−1.47 ± ± 1.44	−2.07 ± ± 2.35	−0.97 ± ± 2.45	−2.51 ± ± 1.51	−1.56 ± ± 2.89	−2.62 ± ± 1.32	−3.05 ± ± 1.55	−2.39 ± ± 3.26	−0.73 ± ± 2.93	−2.52 ± ± 1.45	−1.91 ± ± 2.71
AE, nT	492.6 ± ± 270.2	697.2 ± ± 228.5	482.4 ± ± 230.7	654.3 ± ± 224.2	462.6 ± ± 266.7	608.3 ± ± 226.1	314.7 ± ± 208.8	587.1 ± ± 193.1	523.1 ± ± 254.2	650.2 ± ± 207.5	422.7 ± ± 258.2	603.6 ± ± 217.5

Table 4. Mean values and deviations for $D_{st} \le -100$ nT

Parameter	IND		CIR		Ejecta		MC		Sheath		MC + Ejecta	
	$t=0$	$t=6$	$t=0$	$t=6$	$t=0$	$t=6$	$t=0$	$t=6$	$t=0$	$t=6$	$t=0$	$t=6$
D_{st}, nT	−27.9 ± ± 31.8	−147.9 ± ± 69.8	−20.6 ± ± 25.5	−145.4 ± ± 51.6	−34.9 ± ± 30.9	−136.2 ± ± 39.6	−37.9 ± ± 38.1	−158.1 ± ± 46.5	−20.7 ± ± 31.5	−157.8 ± ± 58.7	−36.1 ± ± 34.1	−146.9 ± ± 47.1
D^*_{st}, nT	−27.6 ± ± 20.3	−134.0 ± ± 20.6	−38.6 ± ± 32.0	−151.0 ± ± 41.4	−53.6 ± ± 35.1	−148.1 ± ± 34.7	−55.2 ± ± 34.2	−178.6 ± ± 42.9	−55.2 ± ± 33.5	−173.8 ± ± 71.8	−54.0 ± ± 34.9	−162.3 ± ± 46.9
$K_p \cdot 10$	56.1 ± ± 14.2	64.4 ± ± 10.8	53.4 ± ± 12.6	64.4 ± ± 10.0	48.0 ± ± 14.9	62.2 ± ± 11.1	62.9 ± ± 13.3	67.2 ± ± 11.1	62.8 ± ± 12.4	66.8 ± ± 11.0	54.3 ± ± 16.0	64.4 ± ± 11.6
B_x, nT	2.4 ± ± 6.9	0.05 ± ± 7.1	0.7 ± ± 7.7	0.6 ± ± 5.7	−0.8 ± ± 4.4	1.2 ± ± 4.6	−0.7 ± ± 7.0	−0.9 ± ± 6.0	−0.4 ± ± 7.1	−1.7 ± ± 7.5	−0.8 ± ± 5.7	0.3 ± ± 5.3
B_y, nT	1.1 ± ± 9.8	3.9 ± ± 9.2	−1.9 ± ± 8.2	0.2 ± ± 10.3	1.9 ± ± 7.3	0.4 ± ± 8.9	−2.7 ± ± 13.1	−0.01 ± ± 9.7	0.3 ± ± 11.4	2.7 ± ± 9.8	−0.1 ± ± 10.5	0.2 ± ± 9.3
B, nT	16.8 ± ± 6.6	14.8 ± ± 5.197	16.1 ± ± 4.5	14.9 ± ± 5.9	12.4 ± ± 3.1	13.4 ± ± 5.2	21.1 ± ± 5.0	17.8 ± ± 4.7	19.0 ± ± 6.7	16.9 ± ± 6.5	16.3 ± ± 5.9	15.2 ± ± 5.4
B_z, nT	−7.1 ± ± 6.3	−4.9 ± ± 4.1	−7.4 ± ± 5.1	−4.2 ± ± 6.8	−4.7 ± ± 5.7	−6.5 ± ± 5.9	−13.5 ± ± 4.5	−9.1 ± ± 9.6	−3.5 ± ± 7.3	−4.9 ± ± 8.9	−8.6 ± ± 6.796	−7.5 ± ± 7.781
n, cm^{-3}	22.4 ± ± 13.7	12.1 ± ± 5.3	23.6 ± ± 12.8	15.5 ± ± 6.9	16.8 ± ± 7.6	11.5 ± ± 8.1	21.3 ± ± 13.0	14.6 ± ± 11.3	30.2 ± ± 22.5	18.9 ± ± 16.2	18.2 ± ± 9.9	12.5 ± ± 9.4
V, km/s	496 ± ± 127	490 ± ± 114	466 ± ± 108	520 ± ± 93	516 ± ± 119	525 ± ± 119	615 ± ± 153	509 ± ± 135	628 ± ± 175	620 ± ± 168	548 ± ± 139	519 ± ± 125
P_k, nPa	8.2 ± ± 5.5	4.4 ± ± 1.8	8.6 ± ± 7.4	6.6 ± ± 2.5	7.5 ± ± 5.4	5.1 ± ± 4.8	12.5 ± ± 7.3	5.9 ± ± 4.6	18.0 ± ± 13.3	12.8 ± ± 13.4	9.1 ± ± 6.5	5.3 ± ± 4.8
T, K, 10^5	1.8 ± ± 1.4	0.99 ± ± 0.5	0.9 ± ± 0.7	2.0 ± ± 1.3	0.6 ± ± 0.7	0.6 ± ± 0.5	1.1 ± ± 1.5	0.3 ± ± 1.9	1.9 ± ± 1.1	1.7 ± ± 0.1	0.8 ± ± 1.0	0.5 ± ± 0.5
P_t, 10^{-2} nPa	6.0 ± ± 7.3	3.7 ± ± 4.3	3.5 ± ± 3.6	3.9 ± ± 2.5	1.3 ± ± 1.3	0.8 ± ± 0.9	1.9 ± ± 1.6	0.7 ± ± 1.0	13.1 ± ± 17.5	4.9 ± ± 5.0	1.5 ± ± 1.4	0.7 ± ± 0.9
β	0.57 ± ± 0.52	0.70 ± ± 0.66	0.38 ± ± 0.41	0.77 ± ± 0.53	0.26 ± ± 0.22	0.15 ± ± 0.13	0.14 ± ± 0.16	0.16 ± ± 0.44	1.88 ± ± 3.79	1.10 ± ± 3.05	0.21 ± ± 0.20	0.15 ± ± 0.31
T/T_{ex}	2.49 ± ± 2.94	2.03 ± ± 1.53	1.27 ± ± 0.75	1.88 ± ± 1.07	0.72 ± ± 0.87	0.59 ± ± 0.72	0.56 ± ± 0.41	0.35 ± ± 0.26	2.09 ± ± 1.82	1.72 ± ± 1.21	0.67 ± ± 0.77	0.50 ± ± 0.60
E_y, mV/m	−3.42 ± ± 2.69	−2.68 ± ± 1.58	−3.09 ± ± 2.41	−1.34 ± ± 2.52	−2.21 ± ± 2.93	−3.02 ± ± 2.55	−7.65 ± ± 4.03	−4.15 ± ± 6.04	−2.81 ± ± 4.54	−2.53 ± ± 4.54	−4.28 ± ± 4.30	−3.46 ± ± 4.30
AE, nT	648.5 ± ± 325.2	742.9 ± ± 233.2	675.8 ± ± 291.1	762.5 ± ± 220.7	667.0 ± ± 382.4	651.3 ± ± 226.2	913.9 ± ± 311.5	824.4 ± ± 272.5	795.9 ± ± 414.3	708.2 ± ± 248.4	772.8 ± ± 374.3	718.8 ± ± 259.4

the time interval after D_{st} index minimum on the recovery phase. In the time interval "0–6" the most fast changes of indices D_{st} and D_{st}^* are observed for Sheath before MC, i.e., the most effective generation of magnetic storms is observed for Sheath before MC, which is consistent with earlier results [9, 15, 16, 29]. The largest distinctions from our previous results are connected with somewhat differing criteria of selection of the solar wind types (first of all, separation of ICME into MC and Ejecta), and with the fact that, instead of criterion $D_{st} < -60$ nT used for magnetic storms in previous papers, in this paper we have used the traditional criterion $D_{st} \le -50$ nT. This coincidence of the results presented above with earlier obtained results is a reliable verification of the method used. At the same time the used DSEA procedure allowed us to obtain some new results.

Separation of ICME in MC and Ejecta has shown that the above-mentioned higher efficiency of Sheath in comparison with MC is observed exclusively in Sheath before MC, while Sheath before Ejecta has approximately the same efficiency as Ejecta. Since the number of MC is approximately an order of magnitude less than the number of Ejecta [22], then for ICME (i.e., without separation of ICME into MC and Ejecta) no difference in efficiency of Sheath and ICME is found. There is rather small difference of parameters in Sheath before MC and Sheath before Ejecta. Therefore, one cannot exclude that the fact mentioned above is connected with distinction of parameters in MC and Ejecta. This issue will a subject of further investigations.

The usual time behavior of parameters B_z (E_y) (with characteristic hour scale of observations), when individual magnetic storm is excited, represents a rather sharp decrease down to a significant negative value and then a sharp increase with typical time of both decrease and increase equal to a few hours. The behavior of D_{st} (D_{st}^*) index on the storm main phase develops according to similar time scenario, but with more gently sloping increase of the index on the recovery phase. Therefore, it seems that the magnetic storm development (behavior of D_{st} (D_{st}^*) index) on the main phase repeats the time behavior of B_z (E_y) with a certain time shift. However, comparison of the average behavior of these parameters at main phase of storm (see Figs. 1, 2, 14, and 15) shows that there is practically no time variation of B_z (E_y) for all types of interplanetary sources. Nevertheless, almost linear decrease of the D_{st} (D_{st}^*) index is observed. This means that the behavior of D_{st} (D_{st}^*) index does not repeat (even with possible shift) the behavior of B_z (E_y), but decreases when negative B_z (E_y) exists, independent of its value, or changes proportionally to integral of B_z (E_y) over time. The latter means that the process of storm generation under negative B_z (E_y) possesses a 'memory' about pre-history. The fact that upon switch-off of negative B_z (E_y) the recovery phase comes in 1–2 h indicates that this 'memory' should be equal to no less than 2 h.

CONCLUSIONS

We have made an analysis of interplanetary sources of 798 magnetic storms with $D_{st} \le -50$ nT using the data archive OMNI for the period 1976–2000. The following large-scale types of the solar wind were considered as sources of the storms: 145 magnetic storms were caused by CIR events, 96 storms were initiated by Sheath (12 magnetic storms were generated by Sheath before MC, Sh_{MC} and 84 magnetic storms by region Sheath before Ejecta, Sh_E); 62 magnetic storms are associated with magnetic clouds MC (50 storms being caused by MC with Sheath and 12 by MC without Sheath); 161 magnetic storms are connected with Ejecta events (115 Ejecta with Sheath and 46 Ejecta without Sheath), sources of the remaining 334 magnetic storms (i.e., 42% out of 798 storms) turn out to be unknown. For the analysis we have applied, presumably for the first time, the double method of superposed epoch analysis in which the instants of magnetic storm onset and of minimum of the D_{st} index were taken as reference times. The following results have been obtained.

1. With large statistical material the well-known fact was confirmed that, independent of the type of interplanetary source, the magnetic storm onset occurs 1–2 h after IMF turn to the south ($B_z < 0$), while both the end of the main phase and the beginning of the recovery phase are observed in 1–2 h after drop of the southward component of the IMF.

2. We have confirmed the result obtained earlier that on the storm main phase the most abrupt changes of indices D_{st} and D_{st}^* are observed for Sheath before MC, i.e., the most effective generation of magnetic storms is observed for Sheath before MC [9, 15, 16, 29]. This effect is better pronounced for stronger magnetic storms. For Sheath before Ejecta no such effect was found, and since the number of Ejecta exceeds the number of MC substantially, for ICME (i.e., without selection of Ejection and MC) this effect is masked and cannot be observed.

3. There are noticeable distinctions between parameters of the solar wind and IMF for various interplanetary sources of magnetic storms, including Ejecta and MC. These distinctions can explain different reactions of the magnetosphere to different types of interplanetary sources. We emphasize that differences in efficiency of MC and Ejecta, as well as of

Sheath before them, are investigated in this paper for the first time.

4. On the main phase of the storm the parameters B_z and E_y decrease near the storm onset, increase near the end of the main phase (minimum of D_{st} and D_{st}^*), and vary slightly between these changes, while D_{st} and D_{st}^* decrease monotonically, approximately proportional to integral of B_z and E_y over time. Such a behavior of the indices is consistent with the assumption that the process of storm generation is not simply related to current values of B_z and E_y, but has a memory about pre-history. Thus, the fact that the 'memory about pre-history' does exist was convincingly demonstrated by us using an independent method.

The obtained results show that the used double method of superposed epoch analysis can be successfully applied for studying the dynamics of parameters on the main phase of storms having different durations. The found tendency that some parameters of the solar wind and IMF demonstrate during strong storms more noticeable deviation from their mean values in comparison with weak and moderate storms can help one to reveal additional geoeffective parameters and to give additional information about mechanisms of magnetic storm generation. This issue will be investigated in further publications.

ACKNOWLEDGMENTS

We thank the authors of the OMNI database (http://omniweb.gsfc.nasa.gov) for opportunity of using it. The work is supported by the Russian Foundation for Basic Research, projects no. 04-02-16131 and no. 07-02-00042, and by the Program of Department of Physical Sciences of the Russian Academy of Sciences no. 15 "Plasma Processes in the Solar System".

REFERENCES

1. Russell, C.T., McPherron, R.L., and Burton, R.K., On the Cause of Magnetic Storms, *J. Geophys. Res.,* 1974, vol. 79, p. 1105.
2. Perreault, P. and Akasofu, S.-I., A Study of Geomagnetic Storms, *Geophys. J. R. Astr. Soc.,* 1978, no. 54, p. 547.
3. Akasofu, S.-I., Energy Coupling between the Solar Wind and the Magnetosphere, *Space Sci. Rev.*, 1981, vol. 28, pp. 121–190.
4. Gonzalez, W.D., Joselyn, J.A., Kamide, Y., et al., What Is a Geomagnetic Storm?, *J. Geophys. Res.*, 1994, vol. 99, no. A4, p. 5771.
5. Dungey, J.W., Interplanetary Magnetic Field and the Auroral Zones, *Phys. Rev. Lett.*, 1961, no. 6, pp. 47–48.
6. Tsurutani, B.T. and Gonzalez, W.D., The Interplanetary Causes of Magnetic Storms, in *Magnetic Storms*, vol. 98 of *Geophys. Monogr. Ser.*, Washington DC: AGU, 1997, p. 77.
7. Gonzalez, W.D., Tsurutani, B.T., and Clua de Gonzalez, A.L., Interplanetary Origin of Geomagnetic Storms, *Space Sci. Rev.*, 1999, vol. 88, p. 529.
8. Yermolaev, Yu.I. and Yermolaev, M.Yu., Statistical Relationships between Solar, Interplanetary, and Geomagnetospheric Disturbances, 1976–2000, *Kosm. Issled.*, 2002, vol. 40, no. 1, pp. 3–16. [Cosmic Research, pp. 1–14].
9. Huttunen, K.E.J. and Koskinen, H.E.J., Importance of Post-Shock Streams and Sheath Region as Drivers of Intense Magnetospheric Storms and High-Latitude Activity, *Ann. Geophys.*, 2004, vol. 22, p. 1729.
10. Alves, M.V., Echer, E., and Gonzalez, W.D., Geoeffectiveness of Corotating Interaction Regions as Measured by D_{st} Index, *J. Geophys. Res.,* 2006, vol. 111, A07S05. doi: 10.1029/2005JA011379.
11. Yermolaev, Yu.I., Yermolaev, M.Yu., and Lodkina, I.G., Comment on "A Statistical Comparison of Solar Wind Sources of Moderate and Intense Geomagnetic Storms at Solar Minimum and Maximum" by J.-C. Zhang, M.W. Liemohn, J.U. Kozyra, M.F. Thomsen, H.A. Elliott, and J.M. 2006, http://arxiv.org/abs/physics/ 0603251.
12. Borovsky, J.E. and Denton, M.H., Differences between CME-Driven Storms and CIR-Driven Storms, *J. Geophys. Res.*, 2006, vol. 111, A07S08. doi: 10.1029/2005JA011447.
13. Denton, M.H. Borovsky, J.E., et al., Geomagnetic Storms Driven by ICME- and CIR-Dominated Solar Wind, *J. Geophys. Res.*, 2006, vol. 111, A07S07. doi: 10.1029/2005JA011436.
14. Huttunen, K.E.J., Koskinen, H.E.J., Karinen, A., and Mursula, K., Asymmetric Development of Magnetospheric Storms during Magnetic Clouds and Sheath Regions, *Geophys. Res. Lett.*, 2006, vol. 33, p. L06107. doi: 10.1029/2005GL024894.
15. Yermolaev, Yu.I., Yermolaev, M.Yu., Lodkina, I.G., and Nikolaeva, N.S., Statistical Investigation of Heliospheric Conditions Resulting in Magnetic Storms, *Kosm. Issled.*, 2007, vol. 45, no. 1, pp. 3–11. [Cosmic Research, pp. 1–9].
16. Yermolaev, Yu.I., Yermolaev, M.Yu., Lodkina, I.G., and Nikolaeva, N.S., Statistical Investigation of Heliospheric Conditions Resulting in Magnetic Storms: 2, *Kosm. Issled.*, 2007, vol. 45, no. 6, pp. 489–498. [Cosmic Research, pp. 461–470].
17. Yermolaev, Yu.I., Yermolaev, M.Yu., Nikolaeva, N.S., and Lodkina, L.G., Interplanetary Conditions for CIR-Induced and MC-Induced Geomagnetic Storms, *Bulg. J. Phys.*, 2007, vol. 34, pp. 128–135.
18. Pulkkinen, T.I. Partamies, N., et al., Differences in Geomagnetic Storms Driven by Magnetic Clouds and ICME Sheath Regions, *Geophys. Res. Lett.*, 2007, vol. 34, p. L02105. doi: 10.1029/2006GL027775.
19. Pulkkinen, T.I., Partamies, N., McPherron, R.L., et al., Comparative Statistical Analysis of Storm Time Activations and Sawtooth Events, *J. Geophys. Res.*, 2007, vol. 112, p. A01205. doi: 10.1029/2006JA012024.
20. Burlaga, L., Sittler, E., Mariani, F., and Schwenn, R., Magnetic Loop behind an Interplanetary Shock: Voyager, Helios, and IMP 8 Observations, *J. Geophys. Res.*, 1981, vol. 86, pp. 6673–6684.

21. Russell, C.T. and Mulligan, T., The True Dimensions of Interplanetary Coronal Mass Ejections, *Adv. Space Res.,* 2002, vol. 29, p. 301.

22. Yermolaev, Yu.I., Nikolaeva, N.S., Lodkina, I.G., and Yermolaev, M.Yu., Catalog of Large-Scale Solar Wind Phenomena during 1976–2000, *Kosm. Issled.,* 2009, vol. 47, no. 2, pp. 99–113. [Cosmic Research, pp. 81–94].

23. Yermolaev, Yu.I., Nikolaeva, N.S., Lodkina, I.G., and Yermolaev, M.Yu., Relative Occurrence Rate and Geoeffectiveness of Large-Scale Types of the Solar Wind, *Kosm. Issled.*, 2010, vol. 48, no. 1, pp. 3–32. [Cosmic Research, pp. 1–30].

24. Huttunen, K.E.J., Koskinen, H.E.J., and Schwenn, R., Variability of Magnetospheric Storms Driven by Different Solar Wind Perturbations, *J. Geophys. Res.*, 2002, vol. 107. doi: 10.1029/2001JA000171.

25. Wu, C.-C. and Lepping, R.P., Effects of Magnetic Clouds on the Occurrence of Geomagnetic Storms: The First 4 Years of Wind, *J. Geophys. Res.,* 2002, vol. 107, p. 1314. doi: 10.1029/2001JA000161.

26. Zhang, J., et al., Solar and Interplanetary Sources of Major Geomagnetic Storms ($D_{st} < -100$ nT) during 1996–2005, *J. Geophys. Res.,* 2007, vol. 112, p. A10102. doi: 10.1029/2007JA012321.

27. Echer, E., Gonzalez, W.D., Tsurutani, B.T., and Gonzalez, A.L., Interplanetary Conditions Causing Intense Geomagnetic Storms ($D_{st} < -100$ nT) during Solar Cycle 23 (1996–2006), *J. Geophys. Res.*, 2008, vol. 113, p. A05221. doi: 10.1029/2007JA012744.

28. Badruddin and Singh, Y.P., Geoeffectiveness of Magnetic Cloud, Shock/Sheath, Interaction Region, High-Speed Stream and Their Combined Occurrence, *Planet. Space Sci.*, 2009, vol. 57, pp. 318–331.

29. Vieira, L.E.A., Gonzalez, W.D., Echer, E., and Tsurutani, B.T., Storm-Intensity Criteria for Several Classes of the Driving Interplanetary Structures, *Sol. Phys.*, 2004, vol. 223, nos. 1-2, pp. 245–258.

30. Turner, N.E., Cramer, W.D., Earles, S.K., and Emery, B.A., Geoefficiency and Energy Partitioning in CIR-Driven and CME-Driven Storms, *J. of Atmosph. and Sol.-Terrest. Phys.*, 2009, vol. 71, pp. 1023–1031.

31. Longden, N., Denton, M.H., and Honary, F., Particle Precipitation during ICME-Driven and CIR-Driven Geomagnetic Storms, *J. Geophys. Res.*, 2008, vol. 113, p. A06205. doi: 10.1029/2007JA012752.

32. Despirak, I.V., Lubchich, A.A., Yahnin, A.G., et al., Development of Substorm Bulges during Different Solar Wind Structures, *Ann. Geophys.*, 2009, vol. 27, no. 5, pp. 1951–1960.

33. McPherron, R.L., Kepko, L., Pulkkinen, T.I., et al., Changes in the Response of the AL Index with Solar Cycle and Epoch within a Corotating Interaction Region, *Ann. Geophys.*, 2009, vol. 27, pp. 3165–3178.

34. Denton, M.H., Thomsen, M.F., Korth, H., et al., Bulk Plasma Properties at Geosynchronous Orbit, *J. Geophys. Res.*, 2005, vol. 110, p. A07223. doi: 10.1029/2004JA010861.

35. Zhang, J.-C., Liemohn, M.W., Kozyra, J.U., et al., A Statistical Comparison of Solar Wind Sources of Moderate and Intense Geomagnetic Storms at Solar Minimum and Maximum, *J. Geophys. Res.,* 2006, vol. 111. doi: 10.1029/2005JA011065.

36. Liemohn, M.W., Zhang, J.-C., Thomsen, M.F., et al., Plasma Properties of Superstorms at Geosynchronous Orbit: How Different Are They?, *Geophys. Res. Lett.*, 2008, vol. 35, p. L06S06. doi: 10.1029/2007GL031717.

37. Ilie, R., Liemohn, M.W., Thomsen, M.F., et al., Influence of Epoch Time Selection on the Results of Superposed Epoch Analysis Using ACE and MPA Data, *J. Geophys. Res.*, 2008, vol. 113, p. A00A14. doi: 10.1029/2008JA013241.

38. Miyoshi, Y. and Kataoka, R., Ring Current Ions and Radiation Belt Electrons during Geomagnetic Storms Driven by Coronal Mass Ejections and Corotating Interaction Regions, *Geophys. Res. Lett.*, 2005, vol. 32, p. L21105. doi: 10.1029/2005GL024590.

39. Badruddin, Transient Perturbations and Their Effects in the Heliosphere, the Geo-Magnetosphere and the Earth's Atmosphere: Space Weather Perspective, *J. Astrophys. Astron.*, 2006, no. 27, p. 209.

40. Taylor, J.R., Lester, M., and Yeoman, T.K., A Superposed Epoch Analysis of Geomagnetic Storms, *Ann. Geophys.*, 1994, vol. 12, pp. 612–624.

41. Maltsev, Y.P., Arykov, A.A., Belova, E.G., et al., Magnetic Flux Redistribution in the Storm Time Magnetosphere, *J. Geophys. Res.*, 1996, vol. 101, p. 7697.

42. Davis, C.J., Wild, M.N., Lockwood, M., and Tulunay, Y.K., Ionospheric and Geomagnetic Responses to Changes in IMF BZ: A Superposed Epoch Study, *Ann. Geophys.*, 1997, vol. 15, pp. 217–230.

43. Yokoyama, N. and Kamide, Y., Statistical Nature of Geomagnetic Storms, *J. Geophys. Res.*, 1997, vol. 102, no. A7, p. 14215.

44. Loewe, C.A. and Prolss, G.W., Classification and Mean Behavior of Magnetic Storms, *J. Geophys. Res.*, 1997, vol. 102, p. 14209.

45. Lyatsky, W. and Tan, A., Solar Wind Disturbances Responsible for Geomagnetic Storms, *J. Geophys. Res.*, 2003, vol. 108, no. A3, p. 1134. doi: 10.1029/2001JA005057.

46. Yermolaev, Yu.I., Yermolaev, M.Yu., Zastenker, G.N., et al., Statistical Studies of Geomagnetic Storm Dependencies on Solar and Interplanetary Events: A Review, *Planet. and Space Science,* 2005, vol. 53, nos. 1/3, pp. 189–196.

47. Vichare, G., Alex, S., and Lakhina, G.S., Some Characteristics of Intense Geomagnetic Storms and Their Energy Budget, *J. Geophys. Res.*, 2005, vol. 110, p. A03204. doi: 10.1029/2004JA010418.

48. Gonzalez, W.D. and Echer, E., A Study on the Peak D_{st} and Peak Negative B_z Relationship during Intense Geomagnetic Storms, *Geophys. Res. Lett.*, 2005, vol. 32, no. 18. doi: 10.1029/2005GL023486.